

Nanoparticles of ferrofluid Fe_3O_4 synthesised by coprecipitation method used in microactuation process

L. PISLARU-DANESCU^a, A. MOREGA^b, G. TELIPAN^{a,*}, V. STOICA^a

^aMicroelectromechanical Department, National Institute for Electrical Engineering ICPE-CA, Bucharest, Romania

^bFaculty of Electrical Engineering, Polytechnic University of Bucharest, Romania

Ferrofluids are a special category of smart nanomaterials in particular magnetically controllable nanofluids. These types of nanofluids are colloidal of magnetic nanoparticles such as Fe_3O_4 stably dispersed in a carrier liquid. The ferrofluid with nanoparticles of Fe_3O_4 was synthesized by co-precipitation method using $\text{FeCl}_3 \cdot 6\text{H}_2\text{O}$ and $\text{FeSO}_4 \cdot 7\text{H}_2\text{O}$ in molar ratio $\text{Fe}^{2+}/\text{Fe}^{3+}=1:2$, dissolved in 300 ml water and treated with NaOH 10% and heated to 80°C. The precipitate Fe_3O_4 was treated with HCl 0.1 n, such as peptizing agent. The precipitate of Fe_3O_4 was magnetic decantation, repeated washed and then dispersed in surfactant acid oleic and inglobed in transformer oil. The proportion nanoparticles Fe_3O_4 /acid oleic/transformer oil was 5/10/85% vol. The purity of the prepared Fe_3O_4 nanoparticles powder was examined by X-ray diffraction. The XRD pattern exhibits the peaks corresponding to Fe_3O_4 cubic with a spinel structure confirmed from hkl Miller indices (220), (311), (400), (511) and (440) with a lattice constant $a=b=c=8.3778 \text{ \AA}$. The medium crystallites size determined with Debye-Scherrer formula was 14 nm. The ferrofluid has dielectric properties, thus, for the frequency 1KHz the relative permittivity was 6,15, the loss tangent was 1.0554 and the impedance was $2.25 \times 10^7 \Omega$.

(Received March 9, 2010; accepted August 12, 2010)

Keywords: Fe_3O_4 , Nanoparticles, Coprecipitation, Microactuation

1. Introduction

A ferrofluid typically consists of ferrimagnetic particles such as Co, FePt, Gd_2O_3 , $\gamma\text{-Fe}_2\text{O}_3$, Fe_3O_4 (approximately 3-15 nm in size) suspended in a nonmagnetic carrier fluid [1,3]. Ferrofluids exhibit a remarkable property: the rheological properties of ferrofluids change on application of an external field. Typical host fluids include hydrocarbon, water, fluorocarbons, esters and silicones [3]. The magnetic materials can be found in a variety of applications that range from microelectronic devices to motors and power distribution system, computer technique, magnetic high-density recording, etc. [4]. Surfacted ferrofluids are formed by magnetic particles coated with surfactant agent (amphiphilic molecules, as: dodecylbenzenesulphonic acid (aprox. C16), lauric acid (LA C12), myristic acid (MA C14) oleic acid (OA C18) in order to prevent their aggregation. Steric repulsion between particles acts as a physical barrier [2,5]. That keeps grains in the solution and stabilizes the colloid. If the particles are dispersed in a nonpolar medium, as transformer oil, one layer of surfactant is needed to form an external hydrophobic layer. The polar head of the surfactant is attached to the surface of the particles and the carbonic chain is in contact with the fluid carrier [6]. Various methods were used for magnetite synthesis: the co-precipitation of Fe^{2+} and Fe^{3+} in alkaline medium [7], electrooxidation of iron in the presence of an amine surfactant [8], hydrothermal process using hydrazine hydrate like surfactant [9]. In this paper we are synthesized the ferrofluid with Fe_3O_4 magnetic nanoparticles by co-precipitation method, using the

surfactant oleic acid and dispersed in transformer oil like carrier fluid.

There was made a PWM signal generator, using two logic devices 4047, Texas Instruments, oscillator connection and positive triggered monostable respectively, having as load the coils L1 and L2. Two power modules are used for load connection, which can be realized with IGBT's transistors. With P1 and P2 variable resistor, we are controlling frequency and duty factor respectively.

2. Experimental

The ferrofluid with nanoparticles of Fe_3O_4 was synthesized by co-precipitation method using $\text{FeCl}_3 \cdot 6\text{H}_2\text{O}$ (99% Merck Germany) and $\text{FeSO}_4 \cdot 7\text{H}_2\text{O}$ (98%, Chimopar Romania), in molar ratio $\text{Fe}^{2+}/\text{Fe}^{3+}=1:2$, dissolved in 300 ml water and treated with NaOH 10%. The mixture was stirring at 80°C for 1 hour. The black color precipitate of Fe_3O_4 was obtained which was washed with deionized water and magnetic decantation until pH 7. At the mixing was added 10 ml HCl 0.1 N for peptization. The mixing was washed and decanted until pH 7 and dried to 90°C and with acetone for water removal. A small part of the powder obtained was analyzed for structural characteristic by X-ray diffraction. The other part of powder was treated with 2 ml acid oleic (99%, -Riedel-de Haen) like surfactant and 5 ml toluene and heated at 90 °C for toluene removal. Finally, the mixing was inglobed in 50 ml oil transformer type UTR 30, under strong stirring for 20 hours for the obtain the ferrofluid.

X-ray analysis was performed with a X Bruker-AXS type D8 ADVANCE diffractometer under $\text{CuK}\alpha$ radiation

(1.5406 Å), 40kV / 40 mA, filter k_{β} of Ni. pas: 0.04 °, measuring time on point: 1 s.

3. Results and discussion

The XRD pattern exhibits the peaks corresponding to Fe₃O₄ cubic with a spinel structure confirmed from hkl Miller indices (220), (311), (400), (511) and (440) with a lattice constant $a=b=c=8.3778$ Å, Fig. 1.

The medium crystallites size determined with Debye-Scherrer formula for the (311) peak was 14 nm.

We have:

$$D = \frac{0.9\lambda}{B \cos \theta} \quad (1)$$

where:

D is grain size, λ is the wavelength of this X-ray $\lambda=0.154059$ nm, B is the full width at half maximum (FWHM) and θ is the half diffraction angle of crystal orientation peak.

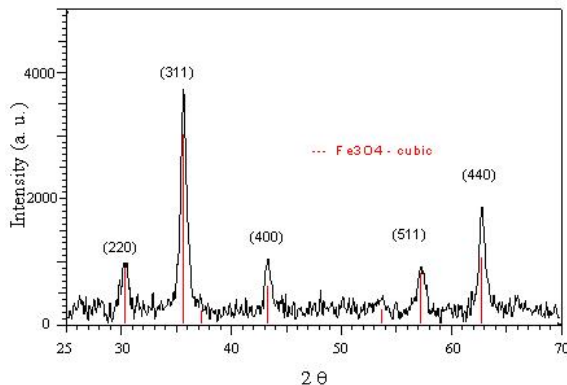


Fig. 1. The Fe₃O₄ XRD pattern and the related peaks.

In the Fig. 2. are presented the hysteresis curves $B = f(H)$ concerning the investigated probes. The measurements were effectuated with the magnetometer VSM 880 (ADE Technologies-USA) from the National Center for the Systems Engineering with Complex Fluids – U.P. Timisoara.

In the Table 1. are indicated the measured values of the saturation magnetization, M_s , and of the saturation magnetic field, H_s (the value of the applied magnetic field at $M=0.95M_s$).

Table 1. The values of the saturation magnetization and the saturation magnetic field.

Probe	The saturation magnetization, M_s		The saturation magnetic field, H_s [kA/m]
	M_s [A/m]	M_s [G]	
Probe	$4.467E^{+3}$	56.132	418.51

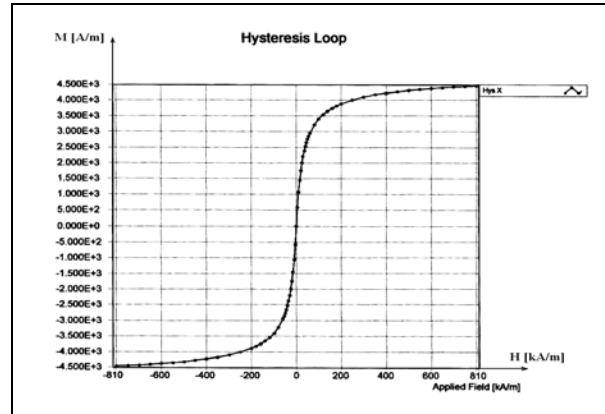


Fig. 2. The hysteresis curve $M(H)$ for the probe.

Based on magnetic ferrofluid we made a microactuator with respect the PWM (pulse width modulation) principle, [12]. Also, this principle is used for the construction of the electronic control system at the microactuator with magnetic ferrofluid. In this way, a short duration impulse determines a low current through the coils L_1 and L_2 of the microactuator and a long duration impulse determines a higher current respectively, as well as a movement in direct ratio to its value.

The main characteristics are: the rectangular waveform, the constant frequency of the output voltage, fixed in the range of the $f = (0 - 24)$ Hz, the possibility of variation of the pulse duty cycle factor between 10% - 90% for the maximal amplitude of $U_{max} = 15V_{cc}$. In Fig. 6 is presented the output PWM rectangular pulse form, for a pulse duty cycle factor of 15%. The PWM generator, Fig. 4, discharges on the microactuator magnetic ferrofluid impedances, L_1 and L_2 . The electromagnetic force developed by the microactuator and implicitly the movement of the magnetic ferrofluid, depends mainly on the coil excitation voltage pulse duty factor $Ku\%$. Also, the maximum amplitude of the excitation voltage is constant, $U_{max} = 15$ V. The RMS value of the current that goes trough the actuator, for a fixed frequency of the PWM voltage, depends mainly on the pulse duty cycle factor. The coils L_1 and L_2 are excited with rectangular waveform, counter phase, in compliance with Fig. 6. The microactuator can work in the “linear mode”, and the pulse duty factor of the voltage, applied on the IGBT transistor gate, T3A and T3B, respectively, Fig. 4., is variable between $k = 10\% - 90\%$, at constant frequency fixed in the range of the $f = (0 - 24)$ Hz. Fig. 5. is showing the microactuator with magnetic ferrofluid during testing. In Fig. 7 and Fig. 8 we can see the thermic profile, after one hour, for the right coil, top view. The maximum temperature value is 45.6 °C.

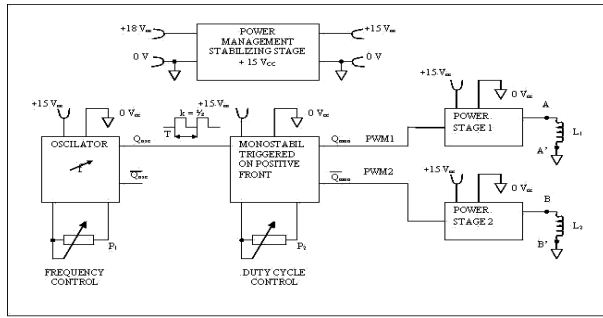


Fig. 3. General view of the PWM signal generator.

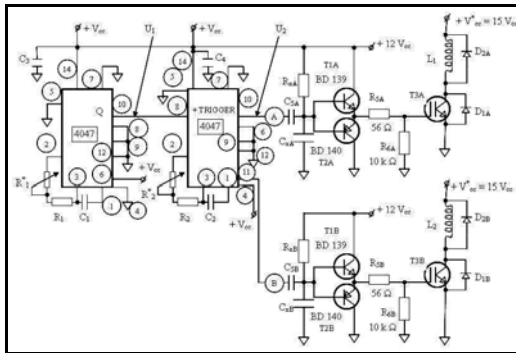


Fig. 4. Signal generator schematic diagram used for the activation of the ferrofluid actuator.



Fig. 5. The microactuator with magnetic ferrofluid during testing.

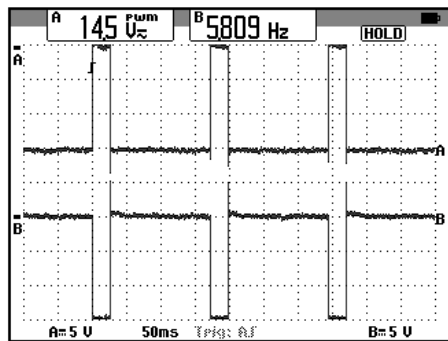


Fig. 6. The output PWM1 and PWM2 rectangular pulse form, for a pulse duty factor of 15 %.

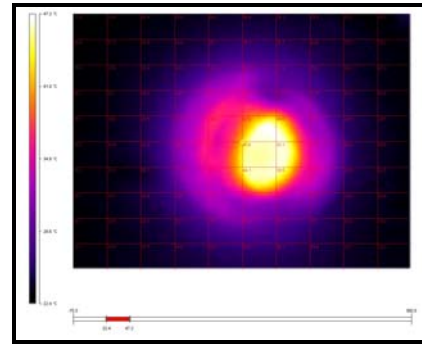


Fig. 7. The thermic profile after one hour, for the right coil, top view.

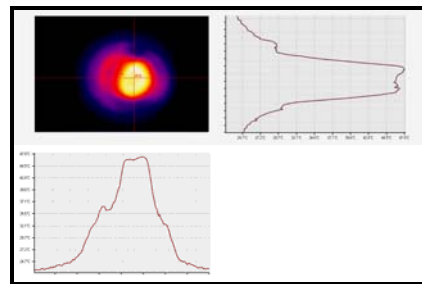
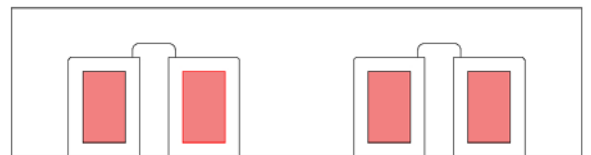


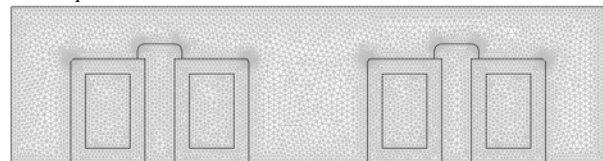
Fig. 8. The thermic profile and spatial temperature distribution after one hour, for the right coil, top view.

4. Mathematical model and numerical simulation results

To overcome the difficulties related to this 3D, unsteady, free surface problem and keeping the physical system within approachable software and hardware limits – still, preserving the outlining processes that occur – several simplifying assumptions are made. We assume that the coils are completely immersed in the magnetic fluid, deep enough such that the waves produced by the magnetic forces are of low amplitude hence the free surface is flat. The magnetically controlled flow is investigated in a 2D cross-sectional domain that comprises the vertical symmetry planes of two coils, Fig. 9.



a. Computational domain.



b. FEM, unstructured mesh made of approx. 14,000 triangular, quadratic, Lagrange elements.

Fig. 9. The computational domain and the discretization mesh used in the numerical simulations.

Fig. 10, depicts the time diagram of the amperturns in the two coils. Their periodicity indicates that the flow may reach a quasi-steady, periodical regime.

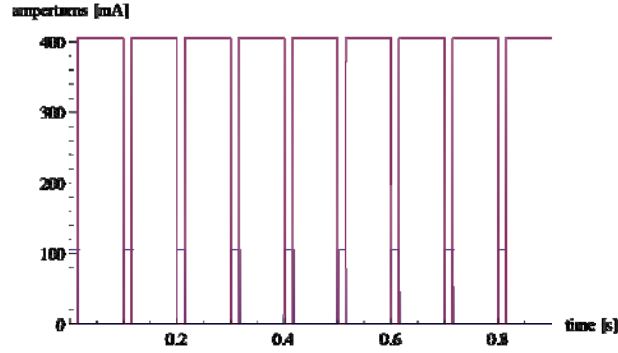


Fig. 10. The amperturns in the two coils.

The mathematical model is made of the following partial differential equations:

Electromagnetic field diffusion (transient, perpendicular induction currents)

$$\sigma \frac{\partial \mathbf{A}_z}{\partial t} + \nabla \times (\mu_0^{-1} \mu_r^{-1} \nabla \times \mathbf{A}_z) = \mathbf{J}_z^e. \quad (2)$$

Momentum balance (Navier-Stokes)

$$\rho \left[\frac{\partial \mathbf{u}}{\partial t} + (\mathbf{u} \cdot \nabla) \mathbf{u} \right] = -\nabla p + \underbrace{\mu (\mathbf{M} \cdot \nabla) \mathbf{H}}_{\mathbf{f}_{mg}} + \mu_f \nabla^2 \mathbf{u} \quad (3)$$

Mass conservation (incompressible flow)

$$\nabla \cdot \mathbf{u} = 0. \quad (4)$$

The quantities in these equations are as follows: \mathbf{u} – velocity; p – pressure; \mathbf{A}_z – magnetic vector field, z -component; \mathbf{J}_z^e external current density (in the coil); \mathbf{f}_{mg} – magnetic body force term, due to the ferrofluid magnetization; σ – electrical conductivity; μ_0 – magnetic permeability (air); μ_f – kinematic viscosity; ρ – mass density.

The magnetic field magnetizes the ferrofluid, and body forces are produced in regions of higher magnetic field gradients. In this study we deal with a superparamagnetic ferrofluid fluid where the influence of the *coercitive magnetic* field intensity, H_c , or the remanent induction, Br , is discarded. The constitutive law for the magnetic field of the magnetic fluid is then

$$\mathbf{B} = \mu_0 \mathbf{H} + \mathbf{M}. \quad (5)$$

Here, \mathbf{M} is the magnetization (in the ferrofluid); \mathbf{H} is the magnetic field strength. The magnetic field produced by

the electrical currents in the coils magnetizes the fluid, and is responsible for the magnetic body forces. The magnetization of the magnetic fluid is approximated here by the analytic formula

$$M = \alpha \operatorname{arctg}(\beta H), \quad (6)$$

with $\alpha = 10^4$ A/m are $\beta = 3 \times 10^{-5}$ m/A empiric constants [1].

Homogeneous initial conditions were assumed. The boundary conditions that close the model are as follows: magnetic insulation (constant A_z) for the boundary of the computational model; no-slip flow conditions for the hydrodynamic part of the problem, except for the upper surface where an open-boundary, normal stress condition is assumed (\mathbf{I} is the unity matrix, η is the dynamic viscosity, \mathbf{n} is the normal to the surface, $(\cdot)^T$ is the transposition operator)

$$\left[-p \mathbf{I} + \eta (\nabla \mathbf{u} + (\nabla \mathbf{u})^T) \right] \cdot \mathbf{n} = 0. \quad (7)$$

The mathematical model was solved numerically by the COMSOL Multiphysics finite element software package [2].

The time integration was performed until the integrated total force per area on the screws heads surfaces reaches a periodic time variation – Fig. 11.

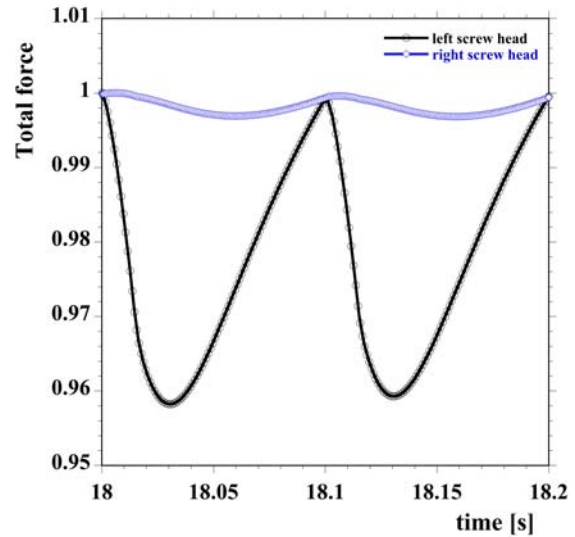


Fig. 11. The magnetic field and the flow by the left coil – nondimensional values.

To plot the two quantities on the same graph, with a satisfactory level of detail, the sign of the integrated total force acting on the left screw head is reversed.

Fig. 12., shows the magnetic field (streamlines) and the flow pattern (velocity through surface color map and arrows) for the coil at the right at a specific moment

during the on-interval (off-interval) of the right coil (left coil).

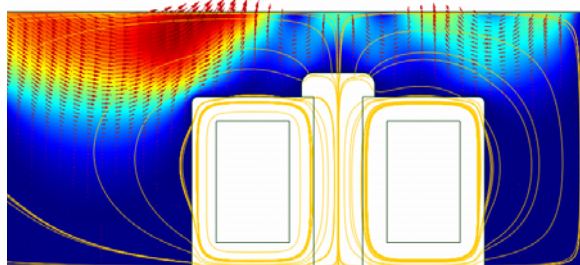


Fig. 12. The magnetic field strength and the flow pattern – the right coil.

Apparently, the flow produced by the magnetic body forces is more important in the regions of higher magnetic field gradients, *e.g.*, above the right coil. The flow pattern indicates that surface waves will be generated, as seen in the experiment. The numerical model presented here may not evidence them, as the upper surface was considered flat.

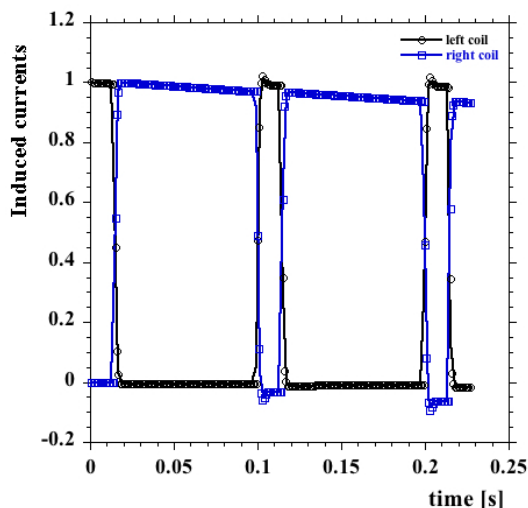


Fig. 13. The induced currents in the coils – non-dimensional values.

Finally, the induced currents (non-dimensional values) in the coils, shortly before reaching the quasi-steady state, are presented in Fig. 13.

5. Conclusions

Was synthesized a ferrofluid with nanoparticles of Fe_3O_4 by co-precipitation method with a molar ratio $\text{Fe}^{2+}/\text{Fe}^{3+}=1:2$. using the surfactant oleic acid and dispersed in transformer oil type UTR 30, like carrier fluid. The X-ray diffraction analysis shows a Fe_3O_4 cubic

phase with a spinel structure and the average crystallite size determined by Debye-Scherrer formula was 14 nm.

By using two coils, L1 and L2, completely immersed in the ferrofluid, can be distinguished the microactuation process. The ferrofluid was synthesized through the method of coprecipitation and the medium crystallite size is 14 nm. The PWM principle is used for the construction of the electronic control system at the actuator with the magnetic ferrofluid. The coils L1 and L2 are excited with a rectangular waveform.

The experiment was realized using a rectangular waveform having the maximum amplitude of 14.5 V, a pulse duty factor of 15 %, and frequency 5.809 Hz.

The thermal profilograma realized after one hour for the right coil, shows a maximum temperature of 45.6°C . By using following partial differential equations like: electromagnetic field diffusion, momental balance, mass conservation, the constitutive law for the magnetic field of the magnetic fluid and approximated law of the magnetization, we make a mathematical model. The COMSOL Multiphysics finite element software package was solved numerically this mathematical model.

Future work will relax the restriction in the mathematical and numerical model.

References

- [1] Vuthichai Ervithayasuporn, Yusuke Kawakami, Journal of Colloid and Interface Science, **332**, 389-393 (2009).
- [2] L. Vekas, D. Bica, O. Marinica, Romanian Report in Physics, **58** (3), 257-267 (2006).
- [3] Koiciro Hayashi, Wataru Sakamoto, Tashinobu Yogo, Journal of Magnetism and Magnetic Materials, **321**, 450-457 (2009).
- [4] Q. Jiang, X. Y. Lang, The Open Nanoscience Journal, **1**, 32-59 (2007).
- [5] S. W. Charles, J. Popplewell, "In Ferromagnetic Material", edited by E.P. Wohlfarth, North-Holland Publishing Company, vol. 2 Amsterdam (1980).
- [6] C. Scherer, A. M. Figueiredo Neto, Brazilian Journal of Physics, **35**(3A), 718-727 (2005).
- [7] Dong-Lin Zhao, Xian-Wei Zeng, Qi-Sheng Xia, Jin-Tian Tang, Journal of Alloys and Compounds, **469**, 215-218 (2009).
- [8] L. Cabrera, S. Gutierrez, N. Menedez, M. P. Morales, P. Herrasti, Electrochimica Acta, **53**, 4336-4441 (2008).
- [9] J. H. Li, R. Y. Hong, H. Z. Li, J. Ding, Y. Zheng, D. G. Wei, Materials Chemistry and Physics, **113**, 140-144 (2009).
- [10] A. M. Morega, M. Morega, F. D. Stoian, S. Holotescu, Proc. of COMSOL Conference, Budapest, 24-25 November 2008.
- [11] COMSOL MultiPhysics, v 3.5a, Comsol AB, (2009).
- [12] Charles Kitchin, Lew Counts, "A Designer's Guide to Instrumentation Amplifiers", 3rd Edition, Analog Devices, printed in USA, 2006.